Nanoscale

ROYAL SOCIETY OF CHEMISTRY

PAPER

View Article Online
View Journal | View Issue

Cite this: *Nanoscale*, 2023, **15**, 2087

Nanosupernova: a new anisotropic nanostructure for SERS†

Kristina Rhee, Anastasiia Tukova, Mohammad Tavakkoli Yaraki and Yuling Wang *

Gold and/or silver nanostars are interesting anisotropic nanoparticles that have been used in surface-enhanced Raman scattering (SERS). In particular SERS nanotags consisting of gold nanostars and Raman reporter molecules have been widely utilised in biosensing and bioimaging. To improve the SERS activity of gold/silver nanostars, this paper details the development of a simple synthesis method that results in the formation of quasi-spherical SERS nanotags and larger highly anisotropic nanoparticles with a novel structure, which we have designated nanosupernova. The resulting SERS nanotags and nanosupernova contain gold/silver nanostars at their core, a self-assembled monolayer of Raman reporter molecules, and a final silver coating. The silver coating is the essential step responsible for the formation of the two types of particles, with incubation time, and type of Raman reporter molecule, the defining factor as to which forms. We discovered that the Raman reporter molecule, 5,5′-dithiobis-(2-nitrobenzoic acid) (DTNB), plays a crucial role in controlling the morphology of nanosupernova. We believe the larger highly anisotropic nanoparticles will open new applications in material sciences and in optical and electronic devices in the future.

Received 26th September 2022,
Accepted 6th January 2023

DOI: 10.1039/d2nr05287c

rsc.li/nanoscale

School of Natural Sciences, Faculty of Science and Engineering, Macquarie University, Ryde, New South Wales 2109, Australia. E-mail: yuling.wang@mq.edu.au

† Electronic supplementary information (ESI) available. See DOI: https://doi.org/10.1039/d2nr05287c

Yuling Wang

Prof. Yuling Wang is an Australian Research Council (ARC) Future Fellow in the School of Natural Sciences at Macquarie University. Yuling completed her PhD at the Chinese Academy of Sciences in 2009. She was then awarded an Alexander von Humboldt (AvH) fellowship (2010) and a German Research Foundation (DFG) fellowship (2012). In 2014, she received the ARC Discovery Early Career Researcher Award (DECRA) fellowship. In 2017, Yuling was appointed as a Senior Lecturer at Macquarie and was promoted to Professor in 2022. Her research focuses on platform technologies that utilize the rationally designed plasmonic nanomaterials and surface-enhanced Raman scattering (SERS) for biomarkers sensing with the aim to enhance in vitro *diagnostics and personalized medicine.*

Introduction

Nanoparticles have been extensively investigated over the past few decades due to their array of important applications including: cancer treatment,[1] biosensing and bioimaging,[2–7] drug delivery,[8] semiconductors,[9] energy production,[10] photocatalysis,[11] and environmental remediation.[12] The biomedical applications of metal nanoparticles have proven to be of great interest to researchers, whom especially favour nanoparticles made from gold, silver and platinum.[13] Gold in particular displays excellent physical and chemical stability, good biocompatibility, and can be easily functionalised with organic and biological molecules.[14,15] Given its unique suitability for biomedical applications the production of gold nanoparticles has been well researched and refined. One common biomedical application of gold nanoparticles is in combination with Raman spectroscopy for the purpose of biosensing and bioimaging.[2]

In the 1970s it was discovered that the Raman spectra intensity of pyridine could be significantly increased if the Raman signal was collected on a roughened silver electrode.[16,17] This process became known as surface-enhanced Raman spectroscopy (SERS) and after further refinement it soon allowed for the detection of analytes at a single molecule resolution.[18] The dramatic enhancement in Raman signal intensity by SERS is thought to be caused by two mechanisms: the chemical effect (sometimes referred to as charge

transfer) and electromagnetic enhancement,[19] with the latter contributing the most.[20] The electromagnetic enhancement is the strongest in "hot-spots" which occur at plasmonic nanostructure junctions and the Raman signal of molecules near these locations are considerably amplified.[21,22] Some biomolecules of interest are Raman active and can therefore be attached to the nanoparticle surface and then directly detected using SERS.[23–25] However, when the target molecules are Raman inactive, it requires that the nanoparticles be labelled with a molecule that exhibits a good and distinct Raman signal or fingerprint for detection.[2] These molecules are often referred to as Raman reporter molecules and nanoparticles functionalised with such molecules referred to as SERS nanotags.

It is known that assembling nanoparticles into dimers and trimers increases SERS signals due to molecular resonance and electromagnetic enhancements.[26] It has also been established that nanoparticles with sharp edges demonstration superior SERS activity due to their anisotropic structure and coupling of the surface plasmon resonance of the particle with the laser excitation.[27] The addition of silver nitrate to gold nanoparticle synthesis has allowed for the fine tuning of SERS characteristics. One such method of nanoparticle synthesis involves using $HAuCl_4$, $AgNO_3$ and reducing agents such as ascorbic acid to create tuneable nanoparticles.[28,29] The proposed mechanism for this process is that the reduction of the $HAuCl_4$ by the ascorbic acid forms the gold core of the particle and the reduction of the $AgNO_3$ by the ascorbic acid allows the $AgNO_3$ to act as a shaping agent which can be manipulated by the chemical ratios and method of mixing.[28] The subsequence nanoparticles can take the form of nanoflowers, nanoshells, nanospheres and nanostars, with the nanostars giving the greatest SERS signal at a laser excitation of 785 nm.[28] Once synthesised metallic nanoparticles can be used for either direct (label-free) or indirect (SERS nanotags) biosensing or bioimaging applications, such as nucleic acid detection,[30] protein biomarkers detection,[31] as well as for *in vitro* detection of cancer biomarkers,[32] and the *ex vivo* imaging of biopsied tissues.[33]

To further enhance the Raman signal of SERS nanotags, a recent innovation has indicated that the addition of a silver coating on nanoparticles functionalised with Raman reporter molecules will dramatically increase the SERS signal. For example, Li *et al.* has reported the addition 20 times Raman enhancement with silver coating on gold nanoparticles functionalized by Raman reporter molecules.[34] In another example, the silver coating of gold nanostars which had been functionalised with a Raman reporter molecule, 4-mercaptobenzoic acid (MBA) gave a significant increase in SERS signal strength compared with the nanostars alone.[35,36]

In addition, interesting applications for larger nanoparticles of around 500 nm have been reported. For example plasmonic nanoantennae have been created by using optical trapping to assemble gold nanobursts (approximately 500 nm in length with sharp and irregular edges) into small clusters within a liquid crystal medium, which has been employed to probe the chemical composition of liquid crystal defect cores, and detect small amounts of organic molecules by SERS.[37] In addition to SERS applications, nanobursts confined within a liquid crystal medium, and collocated with quantum dot-in-rod particles, have been used to study and direct plasmon–exciton interactions.[27] Indeed, there has been significant general interest in distributions of colloidal nanoparticles in liquid crystals because of their optical properties and potential as rearrangeable self-assembling composite materials.[38] This increases the need for unique nanoparticle morphologies with simple synthesis methods to further the field of nanoparticle entrapment within liquid crystal mediums as a method for creating composite materials and for basic research purposes.

To address the need for improved SERS nanotags for biosensing and larger highly anisotropic microparticles for SERS, material science, and basic research applications, we developed a simple synthesis method by coating anisotropic gold/silver nanostars with a thin layer of silver. The proposed synthesis method resulted in the formation of quasi-spherical SERS nanotags (in the presence of any type of Raman reporter molecule) and discovered the formation of larger highly anisotropic nanoparticles with a novel structure only in the presence of 5,5′-dithiobis-(2-nitrobenzoic acid) (DTNB), named nanosupernova, as they resemble an explosion of a star. The SERS nanotags are approximately 110 nm in hydrodynamic size, with a zeta potential of −29.5 ± 8.02 mV, an LSPR peak around 425 nm and a SERS intensity of 6-fold higher than that of gold/silver nanostars coated with Raman reporter molecules without the additional silver layer which the nanotags possess. The nanosupernova are approximately 500–1000 nm in hydrodynamic size, with a zeta potential of −32.5 ± 6.21 mV, an LSPR peak around 425 nm (however broader than the nanotags) and a SERS intensity of 6-fold higher than that of gold/silver nanostars coated with Raman reporter molecules.

Experimental

Reagents and instruments

The reagents HAuCl4, AgNO3, DTNB, 4-mercaptobenzoic acid (MBA), 2,3,5,6-tetrafluoro-4-mercaptobenzoic acid (TFMBA), ascorbic acid and hydroquinone were all purchased from Sigma-Aldrich (Sydney, Australia). Surface-enhanced Raman spectroscopy (SERS) spectra were obtained using a portable Raman microscope (IM-52, Snowy Range Instruments, WY, US) equipped with a 785 nm laser. Each sample was measured six times, with a one second acquisition time, and the average was used for data analysis. UV-Visible spectroscopy (Jasco, Japan) was used to characterise the optical properties of the samples and transmission electron microscopy (TEM, Philips CM10, Eindhoven, The Netherlands) and scanning electron microscopy (SEM, JEOL 6480LA SEM, Peabody, Massachusetts, USA) were used to observe the physical characteristics of the nanoparticles. The samples for TEM and SEM were prepared by adding a 10 μL drop of nanoparticle suspension on top of the carbon-coated copper grid (Zhongjingkeyi Film Technology, Beijing, China), and letting it settle for 3 min before removing the drop with the

filter-paper and drying it overnight. For SEM image, the same TEM grid was used with conducting sticker to connect the grid and the SEM sample holder. Dynamic light scattering (DLS) was used to examine the hydrodynamic size of the samples and zeta-potentials were obtained to examine the surface charge. Both measurements were taken using a Zetasizer Nano (Malvern Panalytica, Malvern, UK).

Gold and silver nanostars synthesis

The synthesis of gold and silver nanostars (Au/AgNSs) was based on the one-pot method proposed by Liu *et al.*[28] Briefly, 1440 μL of 10 mM $HAuCl_4$ and 80 μL of 10 mM $AgNO_3$ were added to a 50 mL centrifuge tube containing 40 mL of Milli-Q water and the tube was vortexed for 30 seconds at 1000 rpm. 240 μL of 100 mM ascorbic acid was added to the tube, the tube quickly sealed and then inverted 2–3 times. The tube was again vortexed for 30 seconds at 1000 rpm and the Au/AgNSs were stored at 4 °C overnight prior to further use (Fig. 1A).

Addition of Raman reporter molecules

1 mL Au/AgNSs were aliquoted into the required number of 1.5 mL centrifuge tubes. 8 μL of 1 mM Raman reporter molecules (DTNB or MBA or TFMBA) were added to each 1 mL Au/AgNSs sample and then incubated with rotation for 2 h at 60 RPM (Fig. 1B). The Au/AgNSs@Ra samples were then centrifuged for 10 min at 6000 rpm, the supernatant removed, and the pellet resuspended in 1 mL of Milli-Q water.

Silver coating

To form the silver coating 90 μL of 10 mM $AgNO_3$ was added to 1 mL samples of Au/AgNSs@DTNB, followed by 30 μL of hydroquinone. The samples were incubated at 21 °C with shaking at 1500 rpm for 10 min, followed by shaking at 750 rpm for 1 h (SERS nanotags) or 12 h (SERS nanosupernova). The synthesis procedure resulted in the formation of nanosupernova reproducibly when followed the precise protocol. The SERS nanotags and SERS nanosupernova were centrifuged for 10 minutes at 6000 rpm, the supernatant removed, and the pellet resuspended in 1000 μL of Milli-Q water and then stored at 4 °C. The synthesis scheme is shown in Fig. 1C.

Nanotags and nanosupernova controls

In the first set of controls three samples were made according to the protocols described above but without the addition of DTNB (Au/AgNSs@Ag). These samples were observed at 1 h and at 12 h to determine if stable silver coated Au/AgNSs formed. In the second set of controls nanotags and nanosupernova were synthesised as per the normal procedure except there was no addition of hydroquinone.

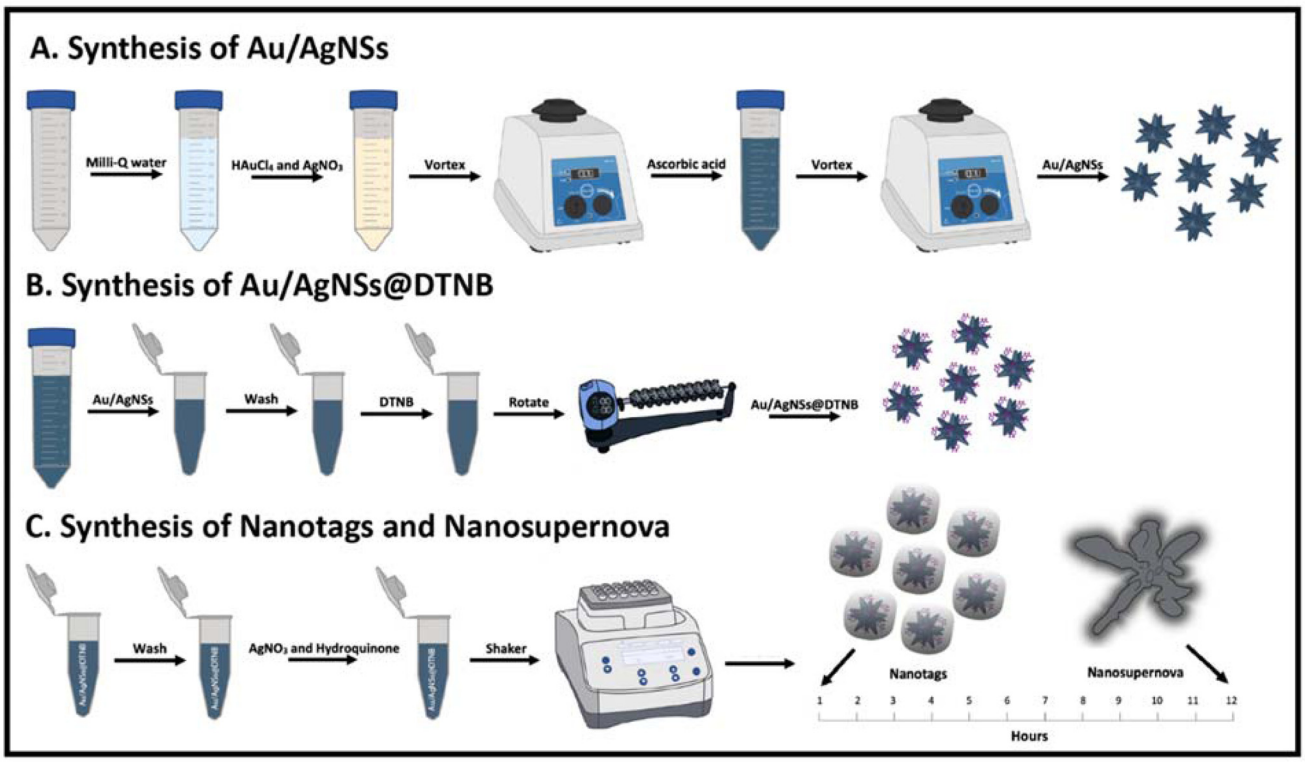

Fig. 1 Schematic illustration of the synthesis. (A): synthesis of Au/AgNSs, (B): synthesis of Au/AgNSs@DTNB, and (C): synthesis of SERS nanotags (Au/AgNSs@DTNB@Ag) and nanosupernova.

Finite-element method simulation

The structures were drawn by Fusion 360 software (Autodesk, USA, CA) after analysis of TEM images of different samples. The enhanced electric field was simulated by solving the governing equations based on Mie theory and using COMSOL Multiphysics software package (see **https://www.comsol.com**), and finite-element method (FEM). The refractive index data for gold and silver were taken from Johnson and Christy's work[39] and Hagemann *et al.*'s work.[40] The surrounding environment was assumed to be water (n = 1.33). Refractive index of DTNB was considered as 1.6. A plane wave linearly polarizing along different directions and propagating perpendicular to the polarization direction at wavelength of 785 nm was set as the source.

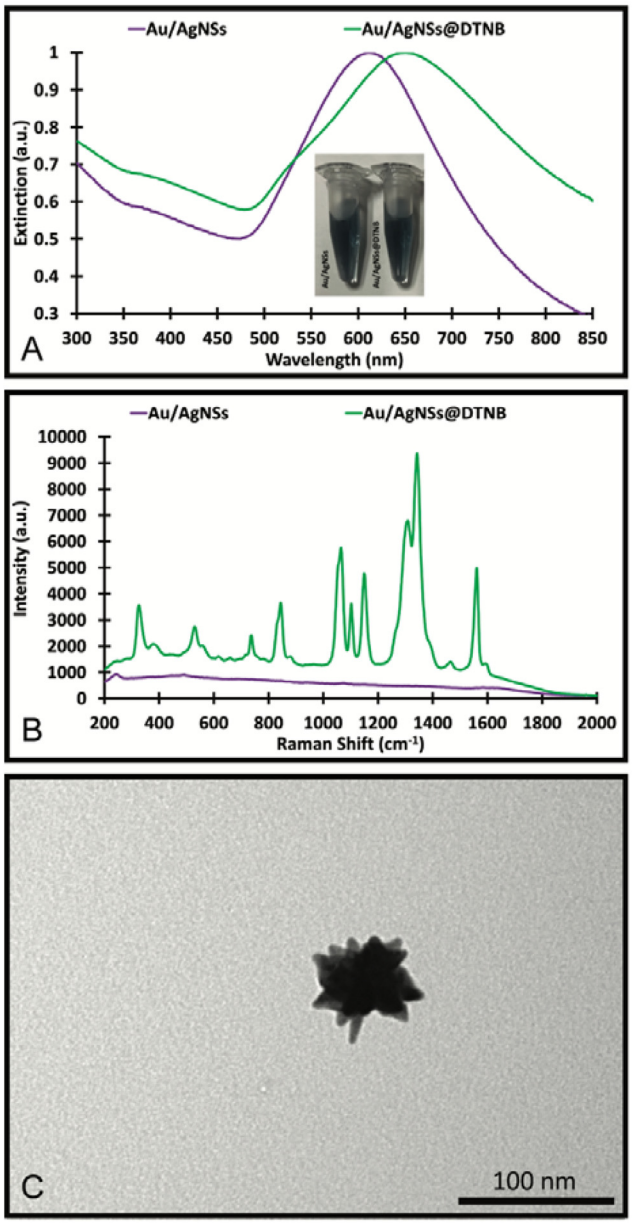

Fig. 2 UV-Visible spectra and photograph of the solution (A), SERS spectra (B) of the Au/AgNSs and Au/AgNSs@DTNB; and the TEM image (C) of the Au/AgNSs.

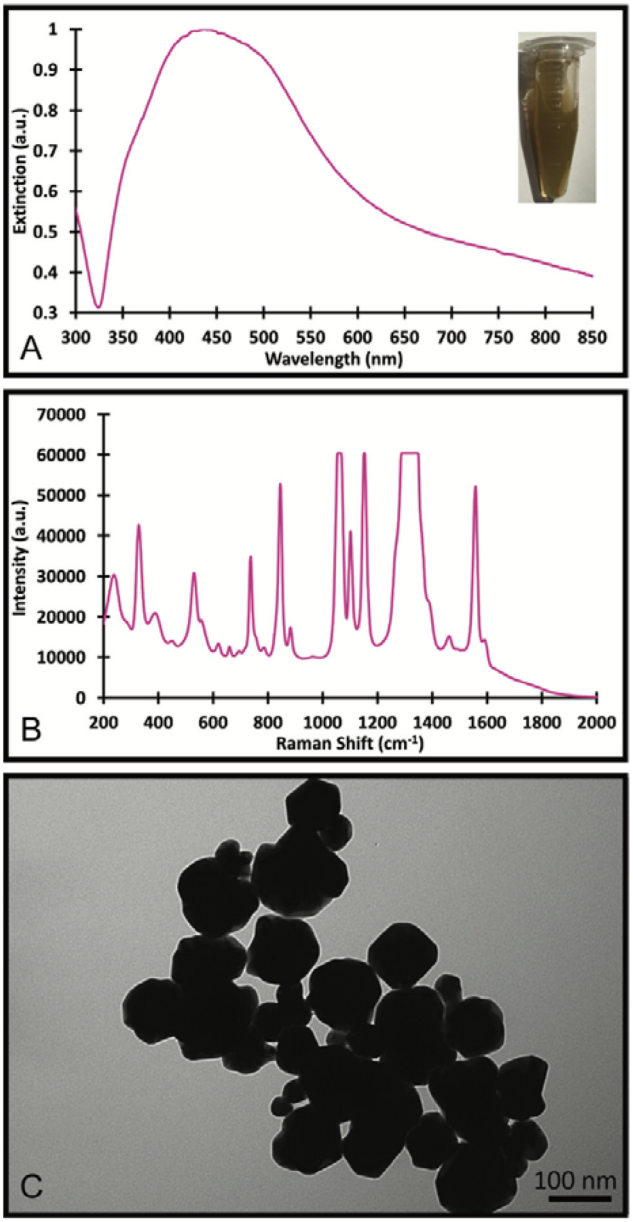

Fig. 3 UV-Visible spectrum and the photograph of the solution (A), SERS spectrum (B) and TEM Image (C) of the SERS nanotags formed with 90 μL of 10 mM $AgNO_3$ and 30 μL of hydroquinone and incubated for 1 h.

Results and discussion

Synthesis and characterisation of Au/AgNSs and Au/AgNSs@DTNB

The Au/AgNSs were synthesised successfully across multiple batches. There was some variability in size and UV-visible peak wavelengths, but this did not appear to affect the synthesis of the final SERS nanotags or nanosupernova. The peak wavelength was around 625 nm (Fig. 2A), and the SERS signal was negligible as expected (Fig. 2B). DLS showed average hydrodynamic size of around 67.70 ± 0.984 nm (Table S1†), meaning the

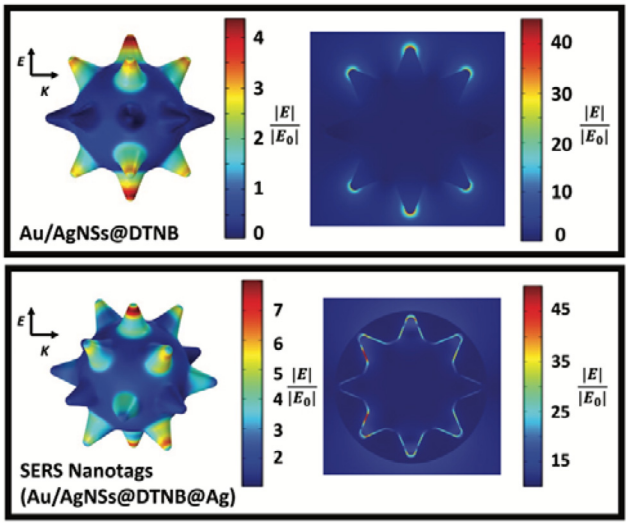

Fig. 4 The simulated enhanced electric field distribution on the surface (top row) and around (bottom row) of Au/AgNSs@DTNB and SERS nanotags (Au/AgNSs@DTNB@Ag). *E* is the polarisation direction and *K* is the propagation direction. The wavelength of the incident light is 785 nm.

population was somewhat polydisperse. The zeta-potential of the Au/AgNSs was −32.3 ± 9.62 mV (Table S1†), indicating stable nanoparticles. The Au/AgNSs have a distinctive blue-green colour in solution (Fig. S3A and B†). The morphology of the Au/AgNSs is shown in Fig. 2C.

Upon incubation with DTNB, the localised surface plasmon peak of the Au/AgNSs@DTNB red-shifted to approximately 650 nm (Fig. 2A) due to increase in refractive index of the surrounding environment of the Au/AgNSs and the distinctive DTNB fingerprint was clearly visible on the SERS spectrum (Fig. 2B, see Table S2† for peaks assignment). This confirms the successful conjugation of DTNB molecules on the surface of the Au/AgNSs. No obvious colour change to the solution was evident upon conjugation of the DTNB molecules (Fig. 2A). No significant change in size occurred after incubation (Table S1†), which is as expected given the monolayer of DTNB would be minor compared with the size of the Au/AgNSs. No significant change in zeta-potential was observed (Table S1†).

Silver coating: nanotags (Au/AgNSs@DTNB@Ag)

The silver coating was formed using $AgNO_3$ and the silver precursor and hydroquinone as the reducing agent. Different synthesis conditions were trialled and are detailed in Fig. S1, S2 and Table S3 of the ESI.†

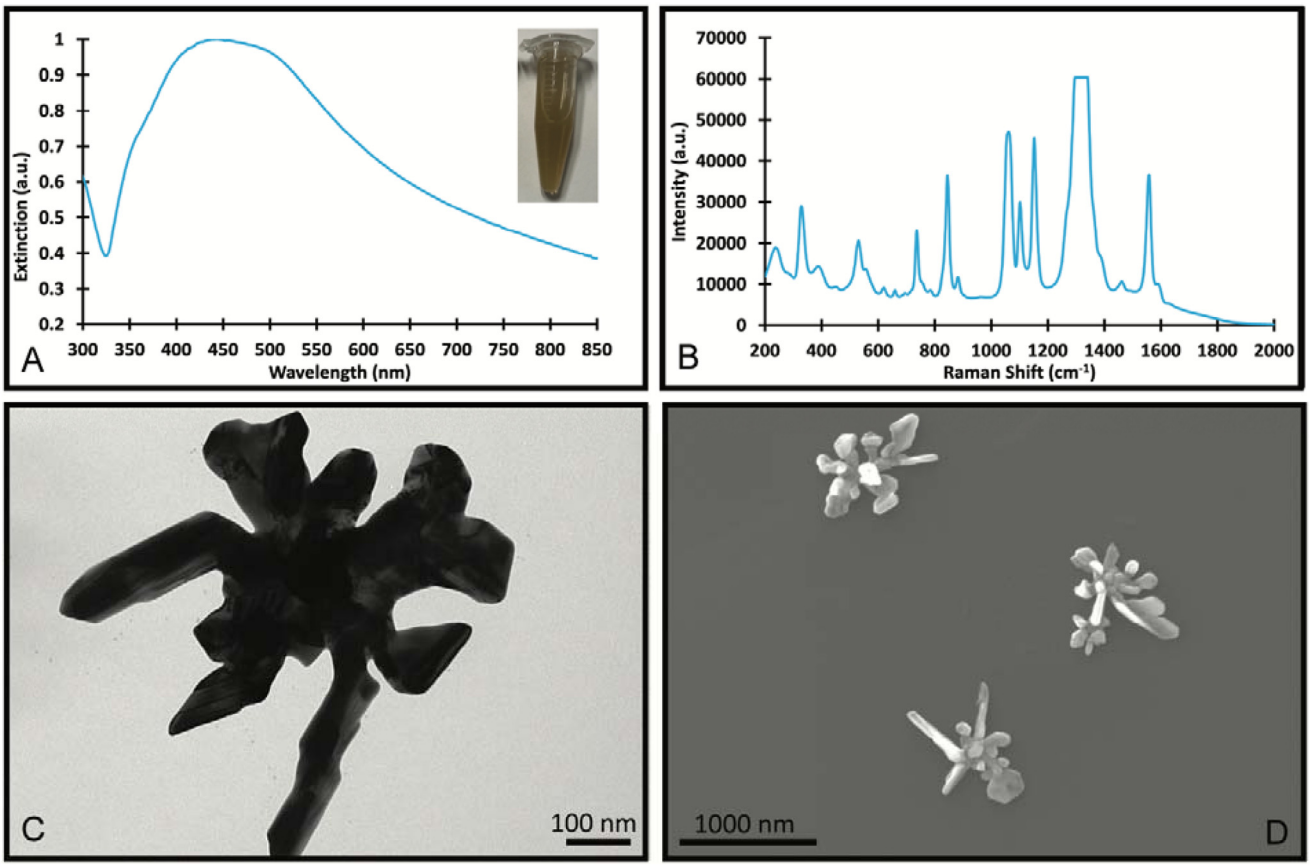

Fig. 5 UV-Visible spectrum (A), SERS spectrum (B), TEM Image (C) and SEM images (D) of the SERS nanosupernova formed with 90 μL of 10 mM $AgNO_3$ and 30 μL of hydroquinone and incubated for 12 h.

It was found that the mixture of 90 μL of $HAuCl_4$ and 80 μL of 10 mM $AgNO_3$ with a 30 μL of hydroquinone and Au/AgNSs@DTNB resulted in the best SERS enhancement (Fig. S1B†). In the synthesis of the SERS nanotags, the colour change did not occur immediately but was achieved by the 1 h mark, where a visible brown/yellow colour change was observed (Fig. 3A). The SERS nanotags had a LSPR peak around 425 nm (Fig. 3A), indicating the formation of silver coating on the Au/AgNSs@DTNB. The SERS nanotags showed enhanced SERS signal (6-fold) compared with Au/AgNSs@DTNB, confirming the positive role of the silver coating on the SERS performance of the as-designed SERS nanotags (Fig. 3B). Comparing the SERS spectra before and after silver coating (Fig. 2B and 3B), we can see that the ratio between the characteristic SERS peaks of DTNB have been changed. This change could be attributed to the effect of silver and possible charge transfer between DTNB molecule and silver, which makes the SERS spectrum of DTNB different from when DTNB is adsorbed on gold.[41,42] The as-synthesized SERS nanotags appear as quasi-circular particles under the TEM (Fig. 3C) and were 108.7 ± 0.8 nm in hydrodynamic size with a good polydispersity index (PDI) of 0.202 (Table S3†). The nanotags had a zeta-potential of −29.5 ± 8.0 mV which indicates that the particles were stable in solution (Table S3†).

To explain the observed SERS enhancement, the electric field distribution around the Au/AgNSs was simulated for before and after the addition of the silver coating. As it can be seen in Fig. 4, the electric field can be improved when a layer of silver has been coated on surface of Au/AgNSs@DTNB. The dramatic increase in SERS signal after the addition of the silver coating is likely due to the surface plasmon coupling resonance effect that takes place between the Au/AgNSs and the thin silver layer. The DTNB layer acts as dielectric and therefore, the metal/dielectric/metal gap plasmon cavity results in the enhanced electric field in the space between the two metals, which leads more DTNB molecules to be excited. This enhanced electric field within the nanotags leads to higher SERS intensity compared with Au/AgNSs@DTNB.[43] This effect has been experimentally shown to occur between gold nanoparticles with a silver coating,[44] and gold nanostars with a silver coating,[35] but to the authors' knowledge this is the first instance of it being demonstrated both experimentally and through simulations between Au/AgNSs and a silver coating.

Nanosupernova

In the synthesis of Au/AgNSs@DTNB@Ag SERS nanotags with maximum SERS intensity (*i.e.*, using 90 μL of $AgNO_3$ with 30 μL of hydroquinone), the incubation time was 1 h. However, if we prolong the shaking time to 12 h, the resulting solution appeared visually identical to the SERS nanotags, where a broader LSPR peak around 425 nm was obtained (Fig. 5A). The as-synthesized nanostructures (nanosupernova) also had excellent SERS signals (Fig. 5B). The TEM and SEM images of these nanostructures revealed that a unique nanosupernova morphology had formed Fig. 5C and D. The additional incubation with shaking appears to have allowed the silver coating to form complex protrusions around the original nanostar core. The timing and speed of the shaking was found to be of particular importance to the formation of these protrusions: with

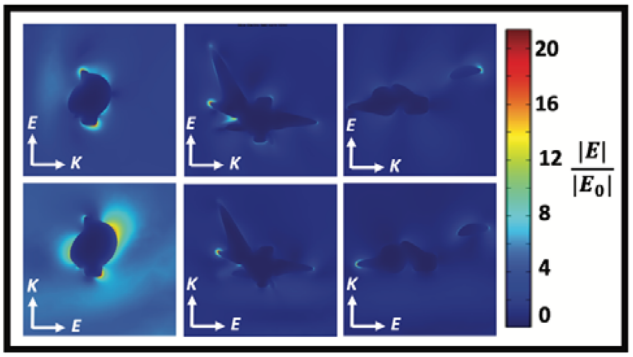

Fig. 6 The simulated enhanced electric field distribution around the Nanosupernova. *E* is the polarisation direction and *K* is the propagation direction. The wavelength of the incident light is 785 nm.

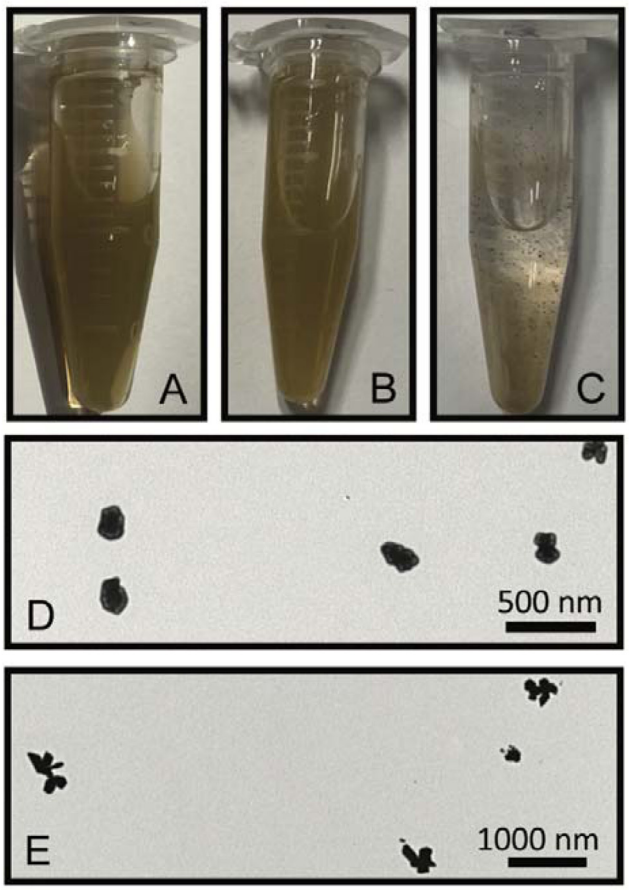

Fig. 7 Photographs of the nanotags (A), nanosupernova (B) and the Au/AgNSs@Ag particles (C). The nanotags and nanosupernova are stable in solution, however when no DTNB is added the particles aggregate. TEM images of particles made using the synthesis method for nanotags (D) and nanosupernova (E), but without the addition of hydroquinone.

the optimal conditions being 10 min of initial shaking at 1500 rpm, followed by shaking for the remainder of the 12 h at 750 rpm (Fig. S3†). Based on the TEM and SEM images the nanosupernova particles are between 500 and 1000 nm, with some protrusions within the 100 nm nanometre range. According to DLS measurements the hydrodynamic diameter of the particles is 428.5 ± 72.2 nm. The zeta-potential of the nanosupernova was −32.5 ± 6.2 mV, which indicates that they are stable in solution. Nanoparticles particles have a morphology that is different to any previously reported in the literature, with the added benefit of an internal SERS reference and excellent SERS signal. The designed nanosupernova have a dramatically enhanced electric field, when excited by incident light at different directions. This demonstrates that the enhanced electric field plays an important role in the SERS enhancement of the nanosupernova. Based on the simulation results, which are shown in Fig. 6 and Fig. S4,† the enhanced electric field distribution depends on the relative orientation between nanosupernova and the incident light, where changing the polarization direction affects the magnitude of enhanced electric field and its distribution, which is expected in anisotropic nanostructures with an asymmetric structure. Performing such a direction-dependent simulations is of great importance since the nanosupernova particles are randomly distributed in the solution and the experimental SERS study in this work has been performed in solution. Our results suggest that the nanosupernova can be excited by 785 nm incident laser, no matter how the particle is orientated in front of laser beam, which demonstrates its great potential to be used as SERS substrate in bio applications. Both Au/AgNSs@DTNB@Ag structures (SERS nanotags and nanosupernova) can be utilised for the multiplex SERS detection, where the strong SERS intensity is favoured for the distinction of Raman peaks from the individual SERS nanotags, leading to improvement of the sensitivity of the SERS biosensor.[45] In particular nanosupernova could be used as internal SERS tag control in the design of planar SERS biosensors.[46,47]

The role of DTNB in the formation of nanosupernova

To understand the formation of nanosupernova, control experiments were performed. Interestingly in the absence of DTNB, the Au/AgNSs@Ag particles aggregated into large visible clumps within 1 h of shaking. Photographs of colloidal solutions comparing the SERS nanotags (Au/AgNSs@DTNB@Ag) (1 h), nanosupernova (Ag/AgNSs@DTNB@Ag) (12 h), and Au/AgNSs@Ag (without DTNB) are shown in Fig. 7A–C. The fact that SERS nanotags and nanosupernova only formed in the presence of a DTNB monolayer, demonstrates that DTNB plays a role in the formation of stable SERS nanotags and nanosupernova.

In another control experiment, hydroquinone was taken out from the synthesis procedure to test if DTNB was

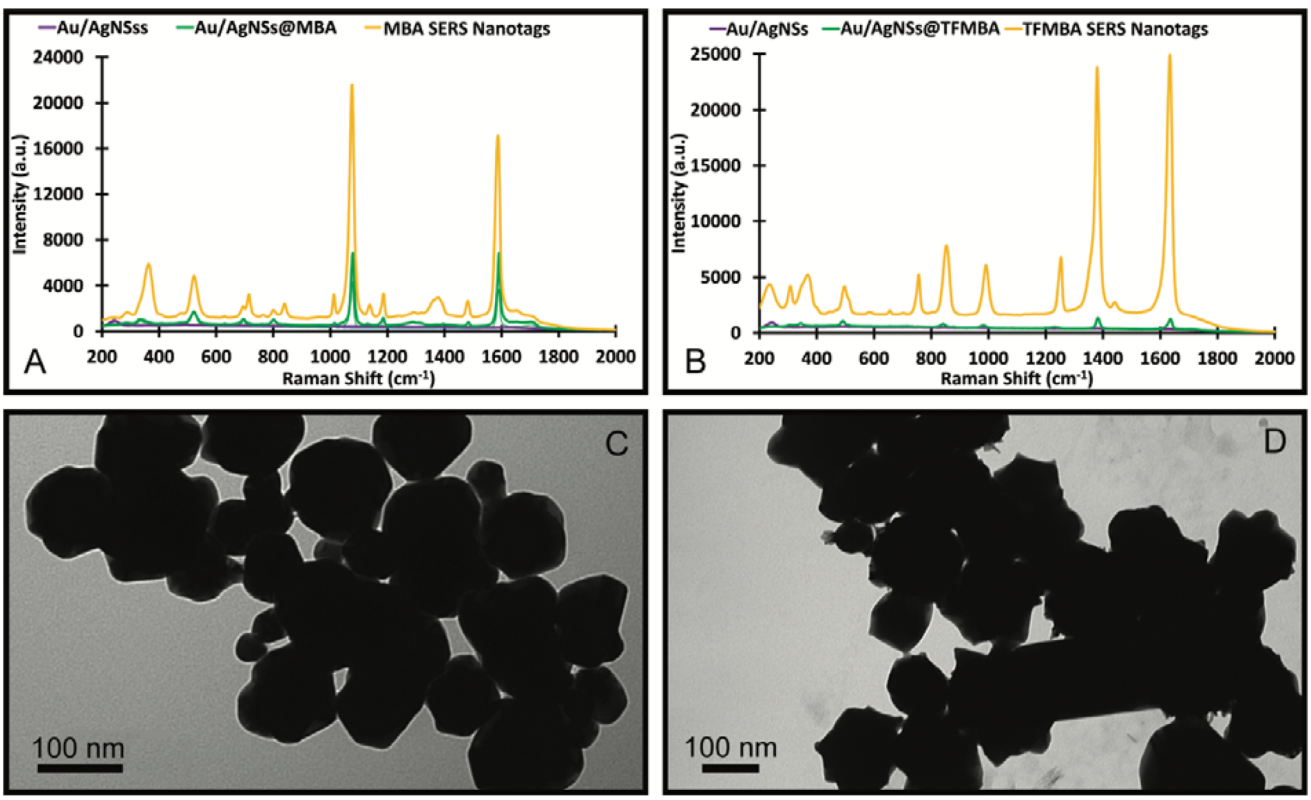

Fig. 8 SERS spectra of the MBA SERS nanotags (A) and TFMBA SERS nanotags (B) made with 30 μL AgNO3 and 30 μL hydroquinone then incubated for 12 hours. The figure includes TEM images of the MBA nanotags (C) and TFMBA nanotags (D).

acting as a reducing agent. As indicated in Fig. 7D, quasi-circular particles (in the absence of hydroquinone) were formed but were larger and less spherical than the SERS nanotags made with hydroquinone (1 h). Under the 12 h reaction, a smaller (appx 300 nm) and less developed protrusions nanosupernova formed in the absence of hydroquinone (Fig. 7E).

Control experiments were also conducted to see if other Raman reporter molecules (MBA and TFMBA) would also enable the formation of nanosupernova. It was found that MBA and TFMBA were able to form SERS nanotags, however under 12 h incubation, which is very similar to that of the DTNB SERS nanotags at 1 h incubation. The MBA nanotags showed an approximately 4-fold SERS intensity increase compared with Au/AgNSs@MBA particles (Fig. 8A). SERS spectrum of TFMBA nanotags was compared with Au/AgNSs@TFMBA particles Fig. (8B). Both MBA and TFMBA SERS nanotags are quasi-spherical in shape and approximately the same size as the DTNB SERS nanotags (1 h incubation), although the TFMBA showed an approximately 10-fold increase in SERS intensity due to the more pointed edges than the MBA and DTNB nanotags (Fig. 8C and D). No nanosupernova structure formed with the MBA and TFMBA as occurred with the DTNB after 12 h of incubation. This supports the notion that DTNB plays a crucial role in the formation of nanosupernova. Although the applications of nanosupernova is out of the scope of this work, we hope to investigate their applications in the future.

Conclusion

This paper has described a simple synthesis method that results in the formation of novel highly anisotropic nanoparticles – nanosupernova with internal SERS reference and excellent SERS signal. We demonstrated that the addition of a silver coating on Au/AgNSs functionalised with one of a variety of Raman reporters (DTNB, MBA and TFMBA) forms SERS nanotags that have a dramatically increased SERS signal when compared to functionalised Au/AgNSs without the silver coating (6-fold that of gold/silver nanostars coated with Raman reporter molecules). In addition, we have discovered that DTNB seems to have inherent reducing capacity and plays a significant role in the morphology of the formation of new nanostructure – nanosupernova, which was also controlled by the reaction time (12 h). The formed nanosupernovas have sizes around 500–1000 nm and show a strong electronic field as demonstrated by FEM simulation. Furthermore, the nanosupernova can be excited by 785 nm incident laser at all orientations in solution which demonstrates its great potential to be used as SERS substrate in colloidal applications. We believe the work detailed in this paper might prove useful for SERS multiplexing applications and of the new anisotropic nanostructure in material science and other optical or electronic applications in future.

Author contributions

All authors contributed to the design of the experiments and analysing the data. K. R., A. T. and M. T. Y. performed the experiments and simulation. K. R. prepared the draft, and the manuscript was finalized through contributions of all authors. All authors have given approval to the final version of the manuscript.

Conflicts of interest

There are no conflicts to declare.

Acknowledgements

This work was supported by the Australian Research Council (ARC) through its Discovery Projects (DP200102004) and Future Fellowship (FT210100737) to Y. W. K. R. acknowledges the scholarship funding support of Macquarie University. The authors gratefully acknowledge the assistance of Grace Rhee in creating the images used for the synthesis schemes. This research was conducted on the land of the Wallumattagal clan of the Dharug nation; we would like to acknowledge these traditional owners of the land and pay our respects to Elders past, present, and emerging.

References

1 M. Tavakkoli Yaraki, B. Liu and Y. N. Tan, *Nano-Micro Lett.*, 2022, **14**, 123.
2 W. Zhang, L. Jiang, J. Piper and Y. Wang, *J. Anal. Test.*, 2018, **2**, 26–44.
3 P. Muhammad, S. Hanif, J. Yan, F. U. Rehman, J. Wang, M. Khan, R. Chung, A. Lee, M. Zheng, Y. Wang and B. Shi, *Nanoscale*, 2020, **12**, 1948–1957.
4 C. Li, Y. Liu, X. Zhou and Y. Wang, *J. Mater. Chem. B*, 2020, **8**, 3582–3589.
5 P. R. Potluri, V. K. Rajendran, A. Sunna and Y. Wang, *Analyst*, 2020, **145**, 2789–2794.
6 J. Wang, K. M. Koo, Y. Wang and M. Trau, *Adv. Sci.*, 2019, **6**, 1900730.
7 J. Wang, K. M. Koo, Y. Wang and M. Trau, *Anal. Chem.*, 2018, **90**, 12698–12705.
8 F. Alexis, E. Pridgen, L. K. Molnar and O. C. Farokhzad, *Mol. Pharm.*, 2008, **5**, 505–515.
9 B. Mangelson, M. Jones, D. Park, C. Shade, G. Schatz and C. Mirkin, *Chem. Mater.*, 2014, **26**, 3818–3824.
10 D. Li, H. Baydoun, C. N. Verani and S. L. Brock, *J. Am. Chem. Soc.*, 2016, **138**, 4006–4009.
11 X. Liu, J. Iocozzia, Y. Wang, X. Cui, Y. Chen, S. Zhao, Z. Li and Z. Lin, *Energy Environ. Sci.*, 2017, **1**, 42–434.
12 I. Khan, K. Saeed and I. Khan, *Arabian J. Chem.*, 2019, **12**, 908–931.

13 S. Ali, A. S. Sharma, W. Ahmad, M. Zareef, M. M. Hassan, A. Viswadevarayalu, T. Jiao, H. Li and Q. Chen, *Crit. Rev. Anal. Chem.*, 2021, **51**, 454–481.
14 V. Amendola, R. Pilot, M. Frasconi, O. M. Maragò and M. A. Iatì, *J. Condens. Matter Phys.*, 2017, **29**, 203002–203002.
15 I. Zare, M. Tavakkoli Yaraki, G. Speranza, A. H. Najafabadi, A. Shourangiz-Haghighi, A. B. Nik, B. B. Manshian, C. Saraiva, S. J. Soenen, M. J. Kogan, J. W. Lee, N. V. Apollo, L. Bernardino, E. Araya, D. Mayer, G. Mao and M. R. Hamblin, *Chem. Soc. Rev.*, 2022, **51**, 2601–2680.
16 M. Fleischmann, P. J. Hendra and A. J. McQuillan, *Chem. Phys. Lett.*, 1974, **26**, 163–166.
17 M. G. Albrecht and J. A. Creighton, *J. Am. Chem. Soc.*, 1977, **99**, 5215–5217.
18 S. Nie and S. R. Emory, *Science*, 1997, **275**, 1102–1106.
19 J. F. Arenas, M. S. Woolley, J. C. Otero and J. I. Marcos, *J. Phys. Chem.*, 1996, **100**, 3199–3206.
20 M. Moskovits, *J. Raman Spectrosc.*, 2005, **36**, 485–496.
21 H.-Y. Chen, M.-H. Lin, C.-Y. Wang, Y.-M. Chang and S. Gwo, *J. Am. Chem. Soc.*, 2015, **137**, 13698–13705.
22 D. Radziuk and H. Moehwald, *Phys. Chem. Chem. Phys.*, 2015, **17**, 2172–2193.
23 J. Wang, K. M. Koo, E. J. H. Wee, Y. Wang and M. Trau, *Nanoscale*, 2017, **9**, 3496–3503.
24 N. Lyu, V. K. Rajendran, R. J. Diefenbach, K. Charles, S. J. Clarke, A. Engel, H. Rizos, M. P. Molloy and Y. Wang, *Nanotheranostics*, 2020, **4**, 224–232.
25 M. A. Tahir, N. E. Dina, H. Cheng, V. K. Valev and L. Zhang, *Nanoscale*, 2021, **13**, 11593–11634.
26 J. P. Camden, J. A. Dieringer, Y. Wang, D. J. Masiello, L. D. Marks, G. C. Schatz and R. P. Van Duyne, *J. Am. Chem. Soc.*, 2008, **130**, 12616–12617.
27 P. J. Ackerman, H. Mundoor, I. I. Smalyukh and J. van de Lagemaat, *ACS Nano*, 2015, **9**, 12392–12400.
28 Y. Liu, N. Lyu, V. K. Rajendran, J. Piper, A. Rodger and Y. Wang, *Anal. Chem.*, 2020, **92**, 5708–5716.
29 A. Tukova, I. C. Kuschnerus, A. Garcia-Bennett, Y. Wang and A. Rodger, *Nanomaterials*, 2021, **11**, 2565.
30 E. J. H. Wee, Y. Wang, S. C.-H. Tsao and M. Trau, *Theranostics*, 2016, **6**, 1506–1513.
31 Y. Wang, R. Vaidyanathan, M. J. A. Shiddiky and M. Trau, *ACS Nano*, 2015, **9**, 6354–6362.
32 U. S. Dinish, G. Balasundaram, Y.-T. Chang and M. Olivo, *Sci. Rep.*, 2014, **4**, 4075.
33 S. Lee, H. Chon, J. Lee, J. Ko, B. H. Chung, D. W. Lim and J. Choo, *Biosens. Bioelectron.*, 2014, **51**, 238–243.
34 J.-J. Li, C. Wu, J. Zhao, G.-J. Weng, J. Zhu and J.-W. Zhao, *Spectrochim. Acta, Part A*, 2018, **204**, 380–387.
35 A. M. Fales and T. Vo-Dinh, *J. Mater. Chem.*, 2015, **3**, 7319–7324.
36 Y. Feng, Y. Wang, H. Wang, T. Chen, Y. Y. Tay, L. Yao, Q. Yan, S. Li and H. Chen, *Small*, 2012, **8**, 246–251.
37 H. Mundoor, T. Lee, D. G. Gann, P. J. Ackerman, B. Senyuk, J. van de Lagemaat and I. I. Smalyukh, *J. Appl. Phys.*, 2014, **116**, 63511.
38 B. Senyuk, D. Glugla and I. I. Smalyukh, *Phys. Rev. E: Stat., Nonlinear, Soft Matter Phys.*, 2013, **88**, 062507–062507.
39 P. B. Johnson and R. W. Christy, *Phys. Rev. B: Solid State*, 1972, **6**, 4370–4379.
40 H. J. Hagemann, W. Gudat and C. Kunz, *J. Opt. Soc. Am.*, 1975, **65**, 742–744.
41 M. Tavakkoli Yaraki, A. Tukova and Y. Wang, *Nanoscale*, 2022, **14**, 15242–15268.
42 N. T. T. Nguyen, M. Tavakkoli Yaraki and Y. Wang, *Mol. Syst. Des. Eng.*, 2023, DOI: **10.1039/d2me00180b**.
43 J.-W. Cho, S.-J. Park, S.-J. Park, Y.-B. Kim, Y.-J. Moon and S.-K. Kim, *Nano Lett.*, 2021, **21**, 3974–3980.
44 C. Duffield, N. Lyu and Y. Wang, *J. Innovative Opt. Health Sci.*, 2021, **14**, 2141007.
45 N. Kim, M. R. Thomas, M. S. Bergholt, I. J. Pence, H. Seong, P. Charchar, N. Todorova, A. Nagelkerke, A. Belessiotis-Richards, D. J. Payne, A. Gelmi, I. Yarovsky and M. M. Stevens, *Nat. Commun.*, 2020, **11**, 207.
46 E. Lenzi, D. Jimenez de Aberasturi and L. M. Liz-Marzán, *ACS Sens.*, 2019, **4**, 1126–1137.
47 W. Shen, X. Lin, C. Jiang, C. Li, H. Lin, J. Huang, S. Wang, G. Liu, X. Yan, Q. Zhong and B. Ren, *Angew. Chem., Int. Ed.*, 2015, **54**, 7308–7312.